Partitioning daily evapotranspiration from a marsh wetland using stable isotopes in a semiarid region

Jing Zhang, Shichun Zhang, Wenguang Zhang, Bo Liu, Chao Gong, Ming Jiang, Xianguo Lv and Lianxi Sheng

ABSTRACT

The hydrological process of evapotranspiration (ET) plays an important role in water circulation in wetlands, and understanding the contributions of wetland ET to local and regional water cycles can help in designing effective wetland management strategies. In this paper, a numerical model, vegetation indexes, and stable isotopes were integrated to partition ET in the Momoge Wetland to understand hydrological processes and calculate the contribution of wetland ET to local hydrological cycling. The results of the non-steady state (NSS) model indicated clear deviation of leaf water enrichment (δ_{Lb}) from an isotopic steady state (ISS) for Phragmites australis, and the model accuracy improved particularly in the early morning and evening when air moisture was highest during the day. The isotopic mass balance showed that E and T contributed approximately 62% and 38% to ET, respectively. Using the estimated proportion of T to ET, in combination for the measured leaf transpiration, total ET was estimated at approximately 8.76 mm d^{-1}. Additionally, the amount of ET clearly changed on an hourly scale, with most primarily occurring at approximately noon. Based on comparison among internationally important wetlands distributed in northeast China, the results in this study are reasonable and will provide theoretical data for wetland water resources management.

Key words | hourly evapotranspiration, marsh, Momoge natural reserve, Phragmites australis, stable isotopes

Jing Zhang
Lianxi Sheng
Key Laboratory of Wetland Ecology and Vegetation
 Restoration,
Northeast Normal University,
5268 Renmin Street, Changchun 130024,
China

Jing Zhang
Shichun Zhang
Wenguang Zhang (corresponding author)
Bo Liu
Chao Gong
Ming Jiang
Xianguo Lv
Key Laboratory of Wetland Ecology and
 Environment,
Northeast Institute of Geography and Agroecology,
Chinese Academy of Sciences,
4888 Shengbei Street, Changchun 130102,
China
E-mail: zhangwenguang@iga.ac.cn

Jing Zhang
School of Biotechnology and Food Engineering,
Changshu Institute of Technology,
99 South Three Ring Road, Changshu 215500,
China

INTRODUCTION

Wetlands are important ecosystems that provide many valuable ecological services, including habitat for species, flood peak attenuation, water purification and climate change mitigation, among others (Woodward & Wui 2001). Hydrological properties are the driving factors of a wetland ecosystem (Mitsch & Gosselink 2007), and particularly, evapotranspiration (ET) plays an important role in the ecosystem water budget and energy balance (Hu et al. 2009) and affects the composition, species diversity and succession of wetland vegetation communities. In wetlands, ET causes major losses of water from the open water surface by evaporation and from the transpiration of emergent plants, which influence regional water cycling (Pauliukonis & Schneider 2001; Chen et al. 2002); therefore, accurate estimates of ET rates for wetland management and water resource assessment are essential. In the past, accurate water balance estimates could not be obtained easily because ET information from vegetation was lacking (Fermor et al. 2001). As a result, the effectiveness of many wetland management practices was low (Peacock & Hess 2004). Currently, worldwide, much research is focused on the contribution of Phragmites australis to ET, including in Australia (Headley et al. 2012), America (Drexler et al. 2008), Spain (Sánchez-Carrillo

et al. 2004), Italy (Borin *et al.* 2011), England (Fermor *et al.* 2001; Peacock & Hess 2004), Germany (Herbst & Kappen 1999), Canada (Lafleur 1990) and China (Zhou & Zhou 2009; Yao *et al.* 2010; Xu *et al.* 2011). Multiple technologies have been used and include the Bowen Ratio Energy Budget (BREB) method (Peacock & Hess 2004), measurements of sap flow (Moro *et al.* 2004), the eddy covariance (EC) method (Zhou & Zhou 2009), remote sensing (Yao *et al.* 2010) and modelling (Herbst & Kappen 1999). Nevertheless, little research has focused on the hourly partitioning of *ET* using a stable isotope method in a *P. australis* marsh wetland.

Motivated by this gap in research, the daily consumptive use of water by *P. australis* and the partitioning of *ET* in the Momoge National Nature Reserve, a semiarid marsh wetland in northeastern China, were determined using a stable isotope method. The objectives in the current study were to (1) investigate the isotopic characteristics of the water pools and fluxes at the site, (2) determine the relative importance of different components to *ET* and the daily

water use by *P. australis* and (3) estimate the daily *ET* distribution on an hourly scale.

MATERIALS AND METHODS

Site and study description

The Momoge National Nature Reserve (45.9359° N, 123.6839° E) is located in the northern Songliao Plain and at the western edge of the Songnen Plain in the northwest of Jilin Province, China. The total area is approximately 1,440 km², of which 90% is wetland. The climate is semiarid with an average annual rainfall of 392 mm. The annual average temperature is approximately 4.2°C. The summers are hot and rainy, and the winters are extremely cold. Eighty per cent of the reserve is composed of the inland saline wetlands that are typical of this region of China (Figure 1) (Ming *et al.* 2007). The sampling site was dominated by a dense stand of *P. australis* of approximately 10 ha (50 m width
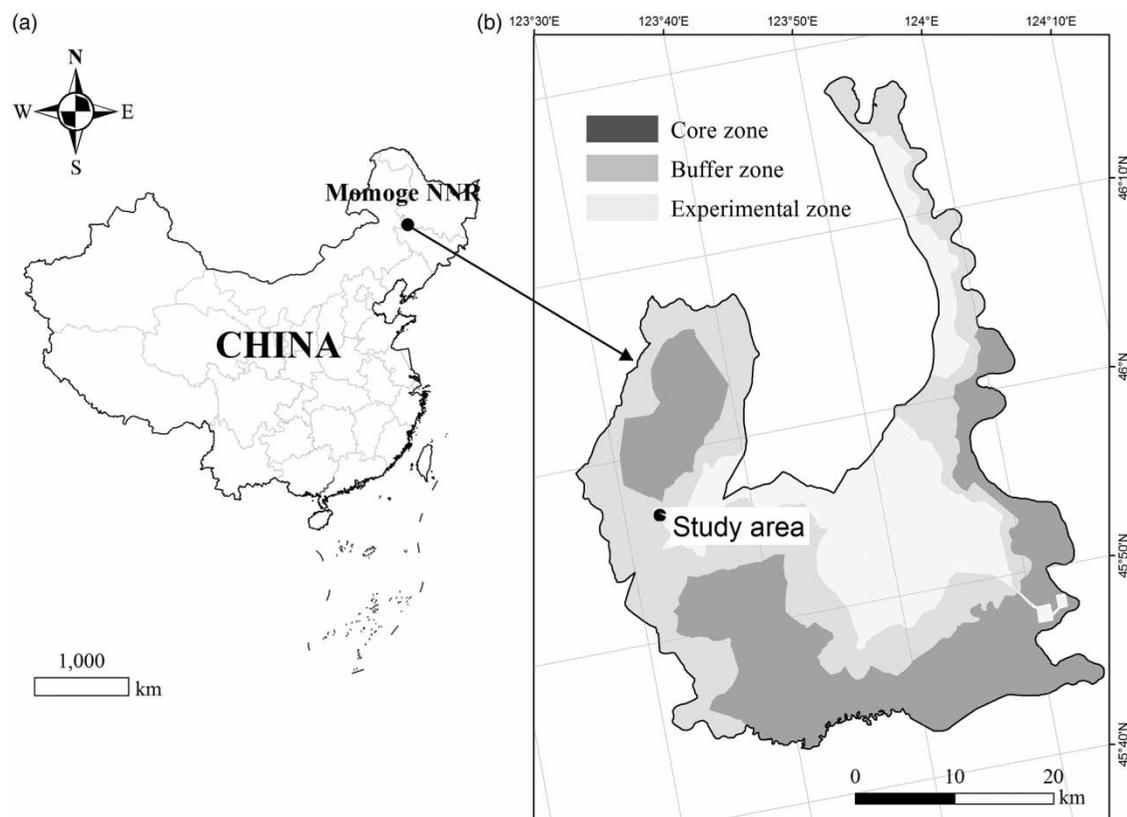

Figure 1 | The location of the Momoge Natural Reserve and the experimental site.

and 2,000 m length), within which all vegetation, leaf area index (LAI) and water depth were measured in a vegetation survey to determine species composition, plant height and plant density.

In this study, many biological and meteorological factors were measured, and the parameters of *P. australis* included the leaf water content (W), specific leaf area (SLA), LAI and leaf-level gas exchange properties. The meteorological factors included water level fluctuation, in addition to air temperature and relative humidity and water surface temperature, which were monitored using an HOBO series temperature and humidity recorder (ProV2, America) and water thermometer, respectively.

The SLA was calculated from the dry weights of 10 pieces of 0.9 cm^2 punched from leaves during the day of sampling. The W was determined from the difference between the fresh and the dry weights of the leaves from five plants and the measured mean SLA of foliage. The LAI was determined by counting the number of individual plants within three replicate 1×1 m plots, sampling 20 individual plants, determining the dry weight and then calculating the leaf areas using dry weights and SLAs. Leaf-level gas exchange properties, including stomatal conductance, transpiration and leaf temperature, were measured using a LI-6400 analyser (Li-Cor Inc., Lincoln, NE, USA) on three leaves of individual plants. Table 1 shows the results.

Sample collection and measurement

In the wetland ecosystem, samples of different water pools were collected five times on two consecutive days, 20th and 21st June 2013, which included surface (0–5 cm) standing water, stem water below the water level and leaf water for *P. australis*, and atmospheric water vapour at three heights (20, 150 and 210 cm) above standing water. Additionally, the atmospheric background water vapour was collected at

the height of 4 m above the ground with no vegetation approximately 100 m from the sampling site.

Standing water samples were collected directly using 2-mL glass vials 0–5 cm below the water level. Stems of *P. australis* were sampled near the roots and below the surface of the standing water. For the collection of leaf samples, the upper and lower leaves of the plants were mixed. Standing water, stem water and leaf water samples were all collected in triplicate, and all samples were sealed immediately with Parafilm in 2-mL glass vials and then frozen below 4°C in the laboratory.

Based on the methods of Helliker *et al.* (2002), atmospheric water vapour was cryogenically captured and analysed for $\delta^{18}O$. Water vapour was collected at three levels above the standing water through a low absorption plastic tube at a flow rate of 0.5 L min^{-1} for 30 min and condensed in a 15-cm-long glass tube placed in a $-80°C$ ethanol/liquid nitrogen bath. The melted water was poured into 2-ml glass vials, which were sealed with Parafilm and stored in a refrigerator until analysis. Each sample was approximately 0.5–1 mL, which is sufficient for $\delta^{18}O$ analysis.

Stem and leaf water samples were extracted in the laboratory using a cryogenic vacuum distillation apparatus (Ehleringer *et al.* 2000). Then, all samples, including water vapour samples, were analysed for $\delta^{18}O$ composition using a Liquid Water Isotope Analyser (Model DLT-100; Los Gatos Research Inc., USA). The precision for $\delta^{18}O$ and δD analyses was better than 0.3‰ and 2‰, respectively (Sturm & Knohl 2010).

Calculation of *T/ET*

In this study, we used the isotopic mass balance of water vapour to determine the contributions of standing water evaporation (E) and transpiration from *P. australis* (T) to total *ET* fluxes in the marsh canopy. Assuming horizontal advection of water vapour was negligible and E and T were the primary sources of vapour in the marsh, the mass balance equations were developed as follows (Lai *et al.* 2006; Bijoor *et al.* 2011):

$$\delta_c = \delta_b f_b + \delta_E f_E + \delta_T f_T \tag{1}$$

$$1 = f_b + f_E + f_T \tag{2}$$

Table 1 | Primary biotic variables and water depth during the sampling period

Leaf water content (mol/m^2)	LAI	Plant height (cm)	Plant density (number/m^2)	Vegetation coverage (%)	Water depth (cm)	SLA (cm/g)
5.4	3.03	203	141	65	85	135.2

where f is defined as the fractional contribution, δ represents the isotopic composition, and the subscripts c, b, E and T represent canopy vapour, background air, standing water evaporation and plant transpiration, respectively. When the isotopic composition of the 'end members' or components (E, T and mixed background vapour) of total canopy vapour are known from measurements or modelling methods, the fractional contributions of each source can be solved by the equations (Phillips & Gregg 2003), and the frequency and range of potential source contributions can be determined. The $\delta^{18}O$ composition of end member δ_c was the water vapour measured at 210 cm above the standing water. The mixed isotopic composition of background air (δ_b) was assumed to be equivalent to the measured $\delta^{18}O$ values of water vapour at the height of 4 m above the ground without vegetation approximately 100 m from the sampling site. The end member δ_E was calculated using the following model (Craig & Gordon 1965):

$$\delta_E = \frac{\delta_e/\alpha_{eq} - h\delta_v - \varepsilon_{eq} - (1-h)\varepsilon_k}{(1-h) + (1-h)\varepsilon_k/1,000} \tag{3}$$

where δ_e is the isotopic composition of liquid water at the surface, δ_v is the isotopic composition of the atmospheric vapour above the water surface, α_{eq} is the temperature-dependent equilibrium fractionation factor, and ε_{eq} is the equilibrium isotopic enrichment defined as $\varepsilon_{eq} = \alpha_{eq} - 1$. For molecular diffusion in air, the kinetic fractionation factor is ε_k, and in this study, the kinetic fractionation factors were approximately 21‰ for oxygen and 11‰ for hydrogen (Bijoor et al. 2011), which included the effects of a turbulent boundary layer (Cappa et al. 2003). The h is relative humidity, which was normalized to the surface temperature of the standing water.

Generally, δ_T is calculated by assuming the attainment of isotopic steady state (ISS), which indicates that the δ_T equals that of the xylem water (δ_s) (Flanagan & Ehleringer 1991). However, plant transpiration is not always in an ISS at time scales of several hours, particularly at night-time (Farquhar & Cernusak 2005; Welp et al. 2008), which could translate into an error in partitioning of ET under the assumption of ISS (Yepez et al. 2005). Thus, the δ_T

from modelled values of leaf water enrichment was calculated at the evaporating sites under non-steady state (NSS) conditions (Δ_{Le}) (Farquhar & Cernusak 2005):

$$\Delta_{Le} = \Delta_{Les} - \frac{\alpha_k\alpha_{eq}}{gw_i}\frac{d\left(W((1-e^{-P})/P)\Delta_{Le}\right)}{dt} \tag{4}$$

where w_i is defined as the water vapour mixing ratio at the temperature of the water at the sites of evaporation (mol mol^{-1}), g is the leaf (stomata and boundary layer) conductance (mol m^{-2} s^{-1}), α_k is the kinetic fractionation factor for molecular diffusion in air, W is the water storage in the leaf lamina (mol m^{-2} leaf), and t is the time in seconds. Δ_{Le} is defined as $\Delta_{Le} = (\delta_{Le}-\delta_s)/(1+\delta_s/1,000)$ (in ‰), where δ_{Le} is the isotopic composition of leaf water at the evaporating sites in δ notation. P is the Péclet number, which describes the ratio of advection to diffusion of enrichment within the leaf. The leaf water enrichment, Δ_{Les}, at the evaporating sites under steady state conditions was calculated as follows (Cernusak et al. 2002):

$$\Delta_{Les} = \varepsilon_{eq} + \varepsilon_k + (\Delta_v - \varepsilon_k) \cdot h \tag{5}$$

where $\Delta_v = (\delta_v-\delta_s)/(1+\delta_s/1,000)$ (in ‰) and is the isotopic enrichment of water vapour relative to that of the source (stem) water and h is the relative humidity normalized to leaf temperature. The isotopic composition of transpiration relative to the source water (Δ_T) was calculated as follows (Farquhar & Cernusak 2005):

$$\Delta_T = \frac{\Delta_{Le} - \Delta_{Les}}{\alpha_k\alpha_{eq}(1-h)} \tag{6}$$

where $\Delta_T = (\delta_T-\delta_s)/(1+\delta_s/1,000)$ (in ‰). Using the estimated fractional contributions of transpiration and measured leaf-level transpiration flux, the total ET flux was calculated as follows:

$$ET = \frac{T}{T/ET} \tag{7}$$

In this estimation, we assumed that each sampling represented the mean of approximately 3 hours.

RESULTS AND DISCUSSION

Isotopic characters

The scatter plot of δD versus δ^{18}O is shown in Figure 2, and the correlation between δD and δ^{18}O was described by δD = 3.53 δ^{18}O − 53.03 ($r^2 = 0.88$, $n = 70$) for the water pools and fluxes in the marsh wetland ecosystem. The data for the liquid water (standing water, stem water and leaf water) were all below the local meteoric water line (LMWL), and the data of vapour were all above the LMWL. These results suggested that the kinetic fractionation of H^{18}O was higher
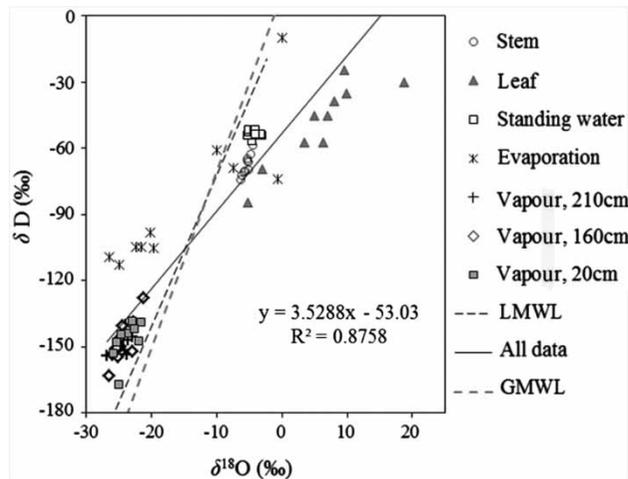
than that of HDO (hydrogen + deuterium + oxygen) and that strong evaporation occurred at the study site because of the dry weather conditions, as indicated by the low slope of the scatter plot. The results for δ^{18}O stable isotope were focused in this study to avoid redundancy. The primary biotic and environmental variables for the two sampling days are shown in Table 2, and the temporal variations of δ^{18}O values of the water pools and fluxes are presented in Figure 3. The δ^{18}O values of the surface standing water were nearly constant, with an arithmetic average ($\pm$standard deviation) of -4.5 ± 0.73‰. The stem water δ^{18}O values (-5.50 ± 0.61‰) of *P. australis* were similar to those of the standing water. However, the leaf water showed a clear isotopic enrichment relative to the source (stem) water (Figure 3).

Daily *ET* partitioning

Using the measured or modelled isotopic end members (i.e., δ_c, δ_b, δ_E and δ_T; Table 2) and the measured leaf-level transpiration, *T/ET* was estimated based on the mass balance equations (Table 3). To evaluate the results of *ET* partitioning, two different methods were used to estimate the ratio of transpiration to *ET*: (1) based on the steady state estimates of δT and the P&G method (ISS method) and (2) based on the NSS estimates δT and the P&G method (NSS method). Using the NSS method, *T/ET* ranged from 0.19 ± 0.12 to 0.67 ± 0.39 with a mean of 0.38 ± 0.18 (Table 4). The ISS and NSS methods produced very similar results, and the

Figure 2 | δ^{18}O–δD relationships for the water pools and fluxes in the wetland ecosystem during the sampling period. The global and local meteoric water line (GMWL) are also shown (grey and black dashed lines, respectively).

Table 2 | Primary biotic and environmental variables at different times during the study

| Time	W (mol m^{-2})	g (mol m^{-2} s^{-1})	w_i (mmol mol^{-1})	T_r (mmol m^{-2} s^{-1})	T_w (°C) (160 cm)	T_a (°C) (160 cm)	RH (%) (160 cm)
20 Jun 0710	5.9	0.005	27.9	0.13	23.7	22.9	68.1
20 Jun 1000	5.5	0.118	33.1	5.70	24.6	28.2	50.7
20 Jun 1230	6.0	0.111	33.3	5.33	26.1	31.6	39.7
20 Jun 1530	5.4	0.081	30.9	3.77	27.3	32.1	43.8
20 Jun 1830	5.9	0.056	18.8	1.58	26.5	25.4	53.5
21 Jun 0700	5.7	0.053	30.2	1.67	23.5	22.8	76.6
21 Jun 0930	3.6	0.054	38.5	2.46	24.4	28.5	54.2
21 Jun 1240	5.6	0.060	39.0	2.70	26.4	31.3	40.8
21 Jun 1530	5.1	0.045	38.9	2.04	27.7	32.0	37.4
21 Jun 1830	5.3	0.027	23.1	0.68	27.3	27.5	41.9
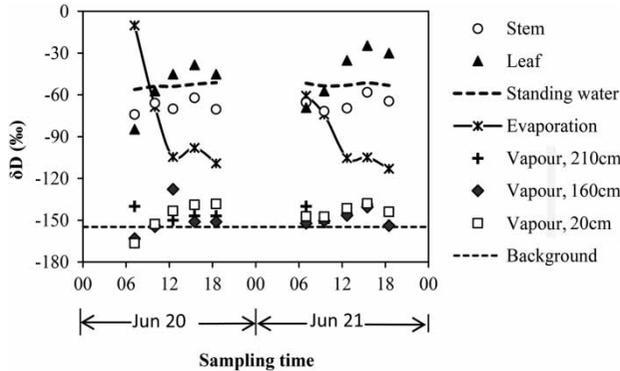
Figure 3 | Temporal variations of $\delta^{18}O$ isotopic composition of water pools and fluxes during the study period.

Table 3 | $\delta^{18}o$ isotopic composition of end members used for distinguishing between evaporation (E) and transpiration (T) in canopy vapour at different times during the study

Time	δ_c	δ_b	δ_E	δ_T	δ_x
20 Jun 0710	−24.00	−27.41	0.05	−12.90	−6.48
20 Jun 1000	−26.82	−27.41	−7.45	−6.83	−5.22
20 Jun 1230	−24.63	−27.41	−22.40	−6.58	−5.78
20 Jun 1530	−23.68	−27.41	−20.19	−5.23	−4.83
20 Jun 1830	−24.30	−27.41	−26.49	−7.13	−5.97
21 Jun 0700	−22.13	−27.41	−9.99	−3.81	−5.36
21 Jun 0930	−24.05	−27.41	−0.68	−8.72	−6.18
21 Jun 1240	−22.86	−27.41	−19.76	−7.46	−5.28
21 Jun 1530	−22.76	−27.41	−21.52	−3.51	−4.49
21 Jun 1830	−23.82	−27.41	−24.90	−20.00	−5.44

Note: The end members were canopy vapour collected at a height of 150 cm above the marsh water surface (δ_c), atmospheric background (δ_b), E from standing water (δ_E), and T from *Phragmites* (δ_T). δT was calculated from the transpiration $\delta^{18}O$ values of *Phragmites* weighted using the measured leaf-level transpiration, LAI and vegetation coverage (Vc). The stem water $\delta^{18}O$ values for *Phragmites* (δ_x) are also shown.

T/ET estimate from the NSS method was approximately 0.05-fold higher than that from the ISS method. Using the estimated *T/ET* from the NSS method, the average estimated total water loss from *E*, *T* and *ET* was 6.29, 2.46 and 8.76 mm d^{-1}, respectively (Figure 4).

Hourly *ET* distribution

The hourly *ET* variation was expressed as a single-peak curve that was relatively low in the morning and evening and high at approximately noon (Figure 4). With the

Table 4 | Estimated *E/ET* and *T_{ph}/ET* fractions using two different methods during the sampling periods: (1) ISS method: from the steady state δ_T estimates and the *E/ET* and *T_{ph}/ET* fractions determined directly by the iterative calculation method proposed by Phillips & Gregg (2003) (herein P&G); (2) NSS method: from the non-steady state δ_T estimates and the P&G method (NSS)

| Time	ISS		NSS	
	E/ET	T/ET	E/ET	T/ET
20 Jun 0700	0.41 ± 0.27	0.59 ± 0.35	0.33 ± 0.21	0.67 ± 0.39
20 Jun 1000	0.56 ± 0.41	0.44 ± 0.36	0.50 ± 0.41	0.50 ± 0.41
20 Jun 1230	0.82 ± 0.49	0.18 ± 0.11	0.81 ± 0.49	0.19 ± 0.12
20 Jun 1530	0.76 ± 0.45	0.24 ± 0.14	0.76 ± 0.45	0.24 ± 0.15
20 Jun 1830	0.78 ± 0.45	0.22 ± 0.02	0.77 ± 0.45	0.23 ± 0.03
21 Jun 0700	0.56 ± 0.34	0.44 ± 0.27	0.58 ± 0.35	0.42 ± 0.25
21 Jun 1000	0.44 ± 0.28	0.56 ± 0.35	0.40 ± 0.25	0.60 ± 0.37
21 Jun 1230	0.75 ± 0.44	0.25 ± 0.15	0.73 ± 0.43	0.27 ± 0.16
21 Jun 1530	0.80 ± 0.48	0.20 ± 0.12	0.81 ± 0.48	0.19 ± 0.12
21 Jun 1830	0.81 ± 0.48	0.19 ± 0.06	0.53 ± 0.31	0.47 ± 0.11
Average	0.67 ± 0.16	0.33 ± 0.16	0.62 ± 0.18	0.38 ± 0.18
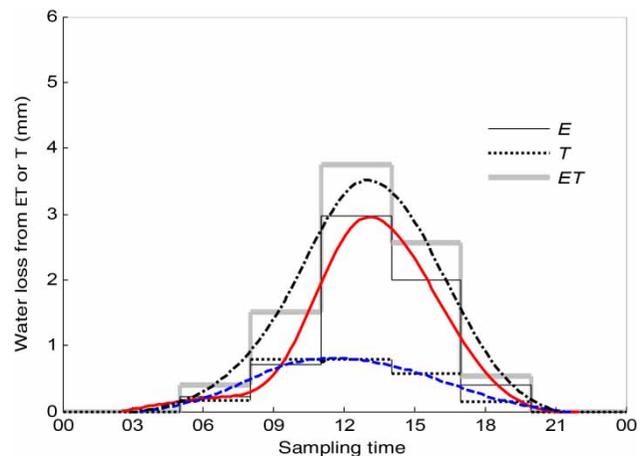
Figure 4 | Water loss from *ET* and transpiration using the estimated *T/ET* during the study periods (the curves show the changes in *ET*, *T* and *E* with time, respectively).

increase in net radiation, air temperature and water surface temperature, the *ET* amount dramatically increased from 0.41 mm in the morning to 3.75 mm at noon, an increase of approximately nine-fold. The *T/ET* ratio change appeared as an 'N' line, with the peak value of approximately 0.53 before noon, the second highest value of approximately 0.43 in the morning, and the minimum of approximately 0.21 at noon. The phenomenon indicated that the transpiration of *P. australis* increased with the increase of

environmental factors (such as net radiation, air temperature and water surface temperature) faster than water evaporation. After noon, the water evaporation decreased faster than *P. australis* transpiration with the descendant coefficients of 1.287 and 0.317, respectively.

The NSS method and model accuracy

Previous studies suggest that not accounting for the NSS of δ_T can introduce large errors in partitioning of *ET* (Yepez *et al.* 2005; Lai *et al.* 2006). In this study, comparisons between the methods for partitioning *ET* showed that the results for ISS and NSS methods were very similar in estimating fractional contributions from *E* and T_{ph} (Table 4). Therefore, although the transpiration was not at an ISS (Table 3; Figure 4), the ISS method also gave reasonable estimations of contributions from *E* and T_{ph}. However, slight discrepancies (less than 5%) were detected for the early morning and evening samplings between the two methods; therefore, consideration of a NSS δ_T in modelling of leaf water for the transitional periods of the day would be beneficial.

Before modelling the NSS δ_T, the leaf water isotopic enrichment model should be validated using the observed values. The temporal variations of the modelled and measured bulk leaf water ^{18}O enrichments (Δ_{Lb}) and the scatter plots of modelled versus measured values showed that in spite of a somewhat underestimate, the modelled Δ_{Lb} agreed well with the observed Δ_{Lb} (Figure 5). Two thresholds can be used to evaluate the departure of leaf water enrichment from a steady state: (1) $\Delta_{Le}-\Delta_{Les}$, the difference between NSS leaf water enrichment at the evaporating sites (Δ_{Le}) and the steady state values (Δ_{Les}) (Welp *et al.* 2008); (2) $\delta T-\delta s$, the difference between transpiration δ_T and the source water δ_s (Harwood *et al.* 1998). The results showed that using the first threshold, either from the forward prediction using Equation (21) in the Farquhar & Cernusak (2005) (herein F&C) model ($\Delta_{Le, F\&C}$) or from the back calculation using the observed bulk leaf water $\Delta^{18}O$ based on Equation (16) in Farquhar & Cernusak (2005) ($\Delta_{Le, back}$), leaf water enrichments were near but deviated from a steady state on both the 20th and 21st June (Figure 5). When using the second threshold, the modelled δ_T always deviated from the observed δ_s, indicating the necessity of modelling the NSS δ_T.
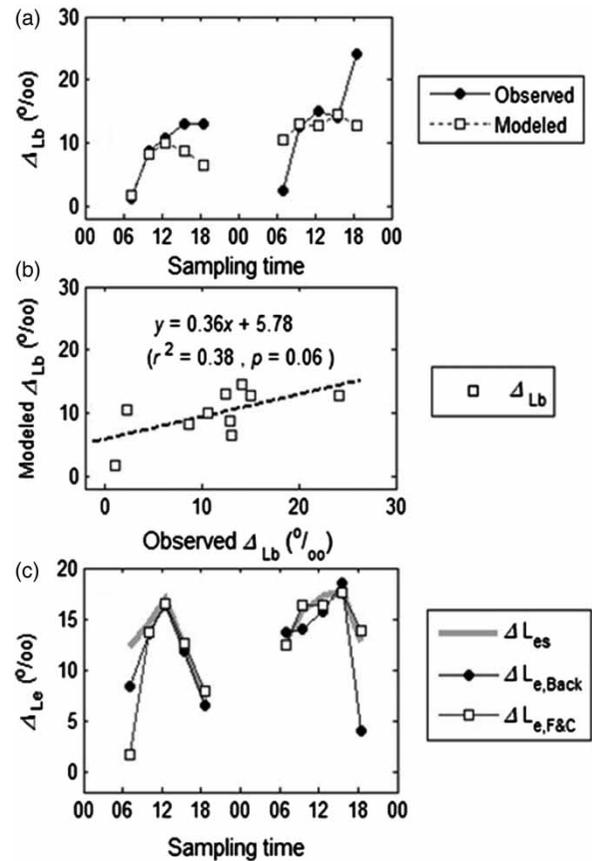

Figure 5 │ Temporal variation and modelled versus observed scatter plots of bulk leaf water enrichment (Δ_{Lb}) and temporal variation of the modelled leaf water enrichment at evaporating sites (Δ_{Le}) during the period of the 20th and 21st June. Δ_{Lb} values were modelled using Equation (21) in Farquhar & Cernusak (2005). Δ_{Le} values were estimated using two approaches, based on a steady state assumption (light grey line): from forward prediction using Equation (22) in Farquhar & Cernusak (2005) (black squares) and from back calculation using the observed Δ_{Lb} values based on Equation (16) in Farquhar & Cernusak (2005) (black solid dots).

The isotopic composition of leaf water was calculated using the F&C model, which considers both the NSS and Péclet effect, and then compared with that of the observed leaf water. Previous studies show that considering the Péclet effect can improve the agreement between modelled and observed leaf water (Farquhar & Cernusak 2005; Welp *et al.* 2008). In this study, the modelled $d\Delta_{Lb}$ values were very consistent with the measured $d\Delta_{Lb}$ values, in spite of the underestimations, particularly in the transition periods of evening and morning (Figure 5). In such transitional periods, the observed Δ_{Lb} values were higher than those of Δ_{Le}, providing support for the argument that isotopic exchanges of $H_2^{18}O$

occur between leaves and the air (Farquhar et al. 2007; Welp et al. 2008).

In this study, both the modelled Δ_{Le} (Figure 5) and the calculated δ_T (Table 3) showed that the leaf transpiration was not at an ISS. The diurnal changes of δ_T values during the study time increased more rapidly than those of δ_x, which is similar to the pattern documented in earlier studies (Harwood et al. 1998; Yakir & Sternberg 2000; Welp et al. 2008). However, notably, the calculated δ_T on the early morning of the 21st June showed very high values during the day, which was caused by the high air humidity ($RH = $ 77.1%) at the time of sampling, because δ_T can be positively correlated with air humidity instantaneously (Lee et al. 2007). Therefore, at this humid site at which the air was prone to saturation in the early morning and evening, the NSS in the modelling of leaf water and transpiration must be considered.

Precision evaluation of ET

Many factors affect ET, including meteorological factors, plant physiological and ecological characteristics, the underlying surface conditions and other factors, with complex variations (Li et al. 2000). In practice, the possible factors are net radiation, air temperature, surface temperature, relative humidity, wind speed and some others (Si et al. 2005). Because of the short experimental time, the results might include some deviation. Therefore, we compared the meteorological data for 9 consecutive sunny days (Table 5). From the contrast of meteorological factors, the relative humidity in the study period was higher than that for the consecutive days in late June and the air temperature was lower by approximately 2.1°C, which resulted in the evaporation difference. The evaporation difference between the experimental period and late June was approximately 3.3%, less than 5%. Thus, the results for the study period were reasonable and credible.

To determine the factors influencing ET in wetlands in northeast China and to further validate the results of this study, we contrasted the ET amount and meteorological factors at wetlands of international importance that are distributed in northeast China (Table 6). Based on the amount of ET, these wetlands were divided into two groups: one group (first group), including the Zhalong and Momoge Wetlands, was distributed in a semiarid area, and the other group (second group) contained the Sanjiang and Panjin Wetlands located in a humid region.

ET is highly dependent upon net radiation (R_n) and air temperature, and peak values of ET often mirror the peaks in R_n or air temperature (Zhou & Zhou 2009). Moreover, the R_n is significantly positively correlated with the sunshine duration. From Table 6, no clear difference is observed in sunshine duration between the two groups; therefore, R_n may not be the primary reason for the difference in

Table 5 | Meteorological factors from the Baicheng station in late June 2013 (the day of precipitation is not shown)

Date	Atmospheric pressure (hpa)	Relative humidity (%)	Air temperature (°C)	Wind speed (m/s)	Sunshine duration (h)	Evaporation (mm)
6–15	984.6	54	24.3	2.6	10.3	13.3
6–16	984.1	52	24	3	7.4	7
6–17	981.6	54	23.9	2.1	11.7	9.7
6–20	989.1	69	20.9	3.1	9.5	8.6
6–21	991.5	62	22.5	2.2	12.7	9.2
6–22	989.3	54	23.8	2.1	13.5	7.9
6–23	985.3	47	25.4	1.8	13.3	9.7
6–24	984.1	52	26.3	3.6	11.8	10.5
6–25	984.4	69	23.1	2.9	4.4	7.1
Average (9 days)	986	57	23.8	2.6	10.5	9.2
Average (study period)	990.3	66	21.7	2.7	11.1	8.9

Note: The data were cited from the China Meteorological Data Sharing Service Network (http://cdc.cma.gov.cn/).

Table 6 │ Comparison of the ET and influencing factors for internationally important wetlands distributed in northeast China (the data are the average values from the same time in late June)

Wetland	Location	Average air temperature (°C)	Relative humidity (%)	Wind speed (m/s)	ET (mm)	Vapour pressure deficit	Net radiation (MJ m^{-2}/d)	Sunshine duration (h)
Zhalong Wetland	46°52′ N, 123°47′ E	29.8	43.2	2.8	8.23	None	None	9.23
Sanjiang Wetland	47°35′ N, 133°31′ E	21.1	62.3	2.2	3.34	9.74	15.2	9.12
Panjin Wetland	41°08′ N, 121°54′ E	20.2	70.4	3.8	3.25	None	None	8.05
Momoge Wetland (this study)	45°56′ N, 123°28′ E	28.1	51.7	4.1	8.76	None	None	8.98

Note: The data were cited from the China Meteorological Data Sharing Service Network (http://cdc.cma.gov.cn/) and other documents (Jia et al. 2007; Sun & Song 2008; Zhou & Zhou 2009; Yao et al. 2010; Zhang et al. 2011).

ET values. However, the air temperature of the first group was dramatically higher than that in the second group. In previous studies, the ET increased with increasing air temperatures, and the correlation coefficient was approximately 0.693. Thus, the air temperature was likely one reason for the differences in ET. Additionally, the relative humidity in the first group was 16.8-fold lower than that in the second group, a clear difference. The relative humidity reflects the influence of the vapour pressure deficit (VPD), with the relative humidity expressed as the ratio between the actual water vapour pressure and saturated vapour pressure at the same temperature (Huang & Liu 2000). Therefore, the air temperature and VPD or relative humidity were likely primary factors that caused the difference in ET between the two groups. The wind speed is a factor that also simultaneously affects the ET amount (Wang et al. 2007; Drexler et al. 2008). In the first group, the ET of the Momoge Wetland was larger than that of the Zhalong Wetland by approximately 0.53 mm/d and the wind speed also increased by approximately 1.3 m/s. In the Panjin Wetland, wind speed promoted and accelerated ET, with a correlation coefficient of approximately 0.477. Thus, overall, air temperature, VPD (or relative humidity) and wind speed are likely the primary factors leading to the differences in ET of wetlands in northeast China.

in the growing season in the semiarid area of the Momoge Natural Reserve. Isotope turbulent mixing relationships, isotopic values of transpired water from plants and those of evaporating water vapour from the wetland were used to estimate the transpiration and evaporation fractions contributing to the total ET. Three important conclusions were derived from this work. (1) The slope of the fitted curve for delta D and delta ^{18}O was approximately 3.53 in the marsh wetland, indicating strong evaporation of surface water in the arid climate (including plant transpiration and water surface evaporation). (2) Using the NSS method, for the proportions of ET, water surface evaporation accounted for approximately 62% and plant transpiration was approximately 38%. The NSS method effectively improved the accuracy of each, particularly in the morning and evening. (3) According to E and T relative contributions and leaf transpiration rate (T_r) measurements, the estimated ET flux was approximately 8.76 mm. In a comparison of wetlands in northeast China, the air temperature, VPD (or relative humidity) and wind speed were likely the primary factors affecting the differences in ET. The water loss from ET is a useful measurement for wetland restoration and wetland water management, and these findings will be helpful in organizing a strict wetland water management plan for semi-arid areas.

CONCLUSIONS

The use of stable isotope techniques to partition ET fluxes into evaporation and transpiration over a marsh wetland was the focus of this work. An experiment was conducted

ACKNOWLEDGEMENTS

supported this study. We thank the anonymous referees for their valuable time.

REFERENCES

Bijoor, N. S., Pataki, D. E., Rocha, A. V. & Goulden, M. L. 2011 The application of delta O-18 and delta D for understanding water pools and fluxes in a Typha marsh. *Plant Cell & Environment* **34** (10), 1761–1775.

Borin, M., Milani, M., Salvato, M. & Toscano, A. 2011 Evaluation of *Phragmites australis* (Cav.) Trin. evapotranspiration in Northern and Southern Italy. *Ecological Engineering* **37** (5), 721–728.

Cappa, C. D., Hendricks, M. B., DePaolo, D. J. & Cohen, R. C. 2003 Isotopic fractionation of water during evaporation. *Journal of Geophysical Research* **108** (D16). doi:10.1029/2003JD003597.

Cernusak, L. A., Pate, J. S. & Farquhar, G. D. 2002 Diurnal variation in the stable isotope composition of water and dry matter in fruiting Lupinus angustifolius under field conditions. *Plant Cell & Environment* **25** (7), 893–907.

Chen, J. H., Kan, C. E., Tan, C. H. & Shih, S. F. 2002 Use of spectral information for wetland evapotranspiration assessment. *Agricultural Water Management* **55**, 239–248.

Craig, H. & Gordon, L. I. 1965 Deuterium and oxygen-18 variations in the ocean and the marine atmosphere. In: *Stable Isotopes in Oceanographic Studies and Paleotemperatures* (E. Tongiorgi, ed.). Laboratory of Geology and Nuclear Science, Pisa, Italy.

Drexler, J. Z., Anderson, F. E. & Snyder, R. L. 2008 Evapotranspiration rates and crop coefficients for a restored marsh in the Sacramento-San Joaquin Delta, California, USA. *Hydrological Processes* **22** (6), 725–735.

Ehleringer, J. R., Roden, J. & Dawson, T. E. 2000 Assessing ecosystem-level water relations through stable isotope ratio analysis. In: *Methods in Ecosystem Science* (O. Sala, R. Jackson, H. A. Mooney & R. Howarth, eds). Springer-Verlag, New York, USA.

Farquhar, G. D. & Cernusak, L. A. 2005 On the isotopic composition of leaf water in the non-steady state. *Functional Plant Biology* **32** (4), 293–303.

Farquhar, G. D., Cernusak, L. A. & Barnes, B. 2007 Heavy water fractionation during transpiration. *Plant Physiology* **143**, 11–18.

Fermor, P. M., Hedges, P. D., Gilbert, J. C. & Gowing, D. J. G. 2001 Reedbed evapotranspiration rates in England. *Hydrological Processes* **15**, 621–631.

Flanagan, L. B. & Ehleringer, J. R. 1991 Stable isotope composition of stem and leaf water-applications to the study of plant water-use. *Functional Ecology* **5** (2), 270–277.

Harwood, K. G., Gillon, J. S., Griffiths, H. & Broadmeadow, M. S. J. 1998 Diurnal variation of $D^{13}CO_2$, $DC^{18}O^{16}O$ and evaporative site enrichment of $dH_2^{18}O$ in Piper aduncum under field conditions in Trinidad. *Plant Cell & Environment* **21** (3), 269–283.

Headley, T. R., Davison, L., Huett, D. O. & Muller, R. 2012 Evapotranspiration from subsurface horizontal flow wetlands planted with *Phragmites australis* in sub-tropical Australia. *Water Research* **46**, 345–354.

Helliker, B. R., Roden, J. S., Cook, C. & Ehleringer, J. R. 2002 A rapid and precise method for sampling and determining the oxygen isotope ratio of atmospheric water vapor. *Rapid Communications in Mass Spectrometry* **16** (10), 929–932.

Herbst, M. & Kappen, L. 1999 The ratio of transpiration versus evaporation in a reed belt as influenced by weather conditions. *Aquatic Botany* **63**, 113–125.

Hu, Z. M., Yu, G. R., Zhou, Y. L., Sun, X. M., Li, Y. N., Shi, P. L., Wang, Y. F., Song, X., Zheng, Z. M., Zhang, L. & Li, S. G. 2009 Partitioning of evapotranspiration and its controls in four grassland ecosystems: application of a two-source model. *Agricultural and Forest Meteorology* **149**, 1410–1420.

Huang, X. & Liu, X. 2000 Study on large scale evaporation model. *Journal of Hehai University* **28** (4), 13–18 (in Chinese).

Jia, Z., Song, C. & Wang, Y. 2007 Studies on evapotranspiration over mire in the Sanjiang Plain. *Climatic and Environmental Research* **12** (4), 496–502 (in Chinese).

Lafleur, P. M. 1990 Evapotranspiration from sedge-dominated wetland surfaces. *Aquatic Botany* **37**, 341–353.

Lai, C. T., Ehleringer, J. R., Bond, B. J. & Paw, U. K. T. 2006 Contributions of evaporation, isotopic non-steady state transpiration and atmospheric mixing on the $d^{18}O$ of water vapour in Pacific Northwest coniferous forests. *Plant Cell & Environment* **29** (1), 77–94.

Lee, X. H., Kim, K. & Smith, R. 2007 Temporal variations of the $^{18}O/^{16}O$ signal of the whole-canopy transpiration in a temperate forest. *Global Biogeochemical Cycles* **21** (3). doi:10.1029/2006gb002871.

Li, L., Zhang, G. & Wang, Q. 2000 Study on evapotranspiration and its impact factors over Yellow River upperstream area. *Advance in Earth Sciences* **15** (3), 256–259 (in Chinese).

Long, D., Gao, Y. & Singh, V. P. 2010 Estimation of daily average net radiation from MODIS data and DEM over the Baiyangdian watershed in North China for clear sky days. *Journal of Hydrology* **388**, 217–233.

Ming, J., Xian-guo, L., Lin-shu, X., Li-juan, C. & Shouzheng, T. 2007 Flood mitigation benefit of wetland soil – a case study in Momoge National Nature Reserve in China. *Ecological Economics* **61** (2–3), 217–223.

Mitsch, W. J. & Gosselink, J. G. 2007 *Wetlands,* 4th edn. John Wiley & Sons Inc., New York, USA.

Moro, M. J., Domingo, F. & López, G. 2004 Seasonal transpiration pattern of *Phragmites australis* in a wetland of semi-arid Spain. *Hydrological Processes* **18** (2), 213–227.

Pauliukonis, N. & Schneider, R. 2001 Temporal patterns in evapotranspiration from lysimeters with three common wetland plant species in the eastern United States. *Aquatic Botany* **71**, 35–46.

Peacock, C. E. & Hess, T. M. 2004 Estimating evapotranspiration from a reed bed using the Bowen ratio energy balance method. *Hydrological Processes* **18** (2), 247–260.

Phillips, D. L. & Gregg, J. W. 2003 Source partitioning using stable isotopes: coping with too many sources. *Oecologia* **136** (2), 261–269.

Sánchez-Carrillo, S., Angeler, D. G., Sánchez-Andrés, R., Alvarez-Cobelas, M. & Garatuza-Payán, J. 2004 Evapotranspiration in semi-arid wetlands: relationships between inundation and the macrophyte-cover: open-water ratio. *Advances in Water Resources* **27** (6), 643–655.

Si, J. H., Feng, Q. & Zhang, X. Y. 2005 Research progress on surveying and calculation of evapotranspiration of plants and its prospects. *Advances in Water Resources* **16** (3), 450–459.

Sturm, P. & Knohl, A. 2010 Water vapor delta H-2 and delta O-18 measurements using off-axis integrated cavity output spectroscopy. *Atmospheric Measurement Techniques* **3** (1), 67–77.

Sun, L. & Song, C. 2008 Evapotranspiration from a freshwater marsh in the Sanjiang Plain, Northeast China. *Journal of Hydrology* **352**, 202–210.

Wang, J. M., Sammis, T. W., Andales, A. A., Simmons, L. J., Gutschick, V. P. & Miller, D. R. 2007 Crop coefficients of open-canopy pecan orchards. *Agriculture Water Management* **88** (1–3), 253–262.

Welp, L. R., Lee, X., Kim, K., Griffis, T. J., Billmark, K. A. & Baker, J. M. 2008 d^{18}O of water vapour, evapotranspiration and the sites of leaf water evaporation in a soybean canopy. *Plant Cell & Environment* **31** (9), 1214–1228.

Woodward, R. T. & Wui, Y.-S. 2001 The economic value of wetland services: a meta-analysis. *Ecological Economy* **37** (2), 257–270.

Xu, S., Ma, T. & Liu, Y. 2011 Application of a multi-cylinder evapotranspirometer method for evapotranspiration measurements in wetlands. *Aquatic Botany* **95**, 45–50.

Yakir, D. & Sternberg, L. D. L. 2000 The use of stable isotopes to study ecosystem gas exchange. *Oecologia* **123** (3), 297–311.

Yao, W., Han, M. & Xu, S. G. 2010 Estimating the regional evapotranspiration in Zhalong wetland with the Two-Source Energy Balance (TSEB) model and landsat7/ETM^{+} images. *Ecological Information* **5**, 348–358.

Yepez, E. A., Huxman, T. E., Ignace, D. D., English, N. B., Weltzin, J. F., Castellanos, A. E. & Williams, D. G. 2005 Dynamics of transpiration and evaporation following a moisture pulse in semiarid grassland: a chamber-based isotope method for partitioning flux components. *Agricultural and Forest Meteorology* **132** (3–4), 359–376.

Zhang, Y., Zheng, X., Wu, C. & Zhang, S. 2011 Experimental study of evapotranspiration from *Phragmites Australis* wetland in Liaohe Estuary. *Advance in Water Science* **22** (3), 351–358 (in Chinese).

Zhou, L. & Zhou, G. 2009 Measurement and modelling of evapotranspiration over a reed (*Phragmites australis*) marsh in Northeast China. *Journal of Hydrology* **372** (1–4), 41–47.